ISBN: 978-3-95450-247-9 ISSN: 2673-5490 doi: 10.18429/JACoW-IPAC2024-MOPC37

MECHANICAL ANALYSIS AND DESIGN FOR THE LCLS-II-HE SOFT X-RAY UNDULATOR RECONFIGURATION*

P. Mallon†, D. Arbelaez, K. Hanzel, M. Kota, K. McCombs, K. Ray
Lawrence Berkeley National Laboratory, Berkeley, U.S.A.

Abstract

As a part of the High Energy upgrade to the Linac Coherent Light Source II (LCLS-II-HE) at SLAC, LBNL is responsible for the update of the undulators of the Soft X-Ray (SXR) line. In order to span the required photon energy range, the LCLS-II-HE SXR undulators (SXU) require a longer magnet period length when compared to the original LCLS-II undulators. This increased magnet period leads to higher magnetic force, requiring updates to certain elements of the design. In contrast, many elements can safely remain unchanged. This paper details the updates and analyses performed to support the adaptation to HE-SXU.

INTRODUCTION

The world's first Hard X-Ray Free Electron Laser (XFEL), the Linac Coherent Light Source (LCLS), was recently upgraded as part of the LCLS-II project. The LCLS-II upgrade includes the addition of a 4 GeV superconducting RF linac and two new variable gap undulator lines. LBNL was involved in the design and delivery of the variable gap undulators for the Soft X-Ray (SXR) and Hard X-Ray (HXR) lines for LCLS-II [1]. A more recent upgrade to the LCLS is currently taking place as part of the LCLS-II-HE project [2]. As part of this project, the superconducting linac energy will be increased to 8 GeV. Due to the increased energy, the SXR undulators (SXU) require longer magnetic period to span the required photon energy range. LBNL is responsible for the design and procurement of components required for updating the SXR undulator line.

LCLS-II SOFT X-RAY UNDULATOR OVERVIEW

The LCLS-II SXR undulator is a tunable gap insertion device. The upper and lower magnet modules are mounted to stiff aluminum strongbacks, which themselves are mounted to the drive system through flexure plates. The drive system is then connected to the support frame, which provides rigidity to the rest of the assembly. A view of a single undulator unit is shown in Fig. 1. The key components requiring replacement during the upgrade to HE-SXU are the magnet modules and compensation springs. For the remainder of the components, the goal is to reuse as much as possible without modification.

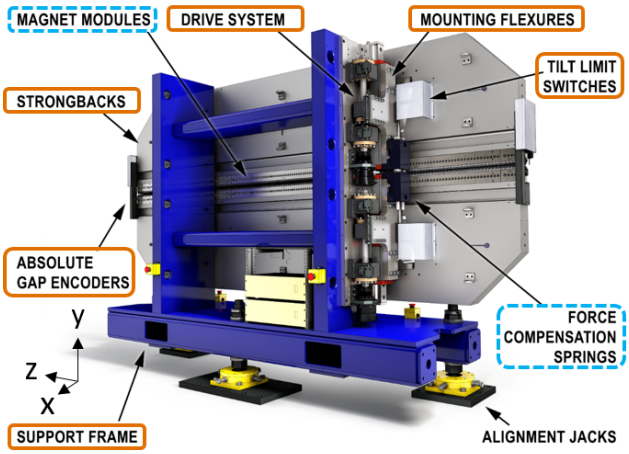

Figure 1: The LCLS-II undulator showing key components. For HE-SXU, the magnet modules and the compensation spring stacks require replacement.

MECHANICAL SYSTEM ANALYSIS

As a part of this upgrade, the attractive force present between the upper and lower magnet modules of the undulator at the smallest gap is increasing by more than 30 % from 70 kN to 92 kN. Figure 2 shows a comparison of the HE-SXU and current SXU attractive force per drive system as a function of gap. The goal of this paper is to show that the mechanical system can be used with modifications. The analyses that were performed to assess the need for modification were guided by the physics requirements listed in Table 1. The physics requirement for maximum gap variation ensures that phase errors due to the deformation of the strongbacks, which is driven by the magnetic force, remain below allowable limits. The roll between the strongbacks (relative rotation about the z-xis) and the centerline offset between the strongbacks (shift of the strongback position relative to the beam centerline) are alignment requirements that are also affected by the increase in magnetic force.

Table 1: Relevant Physics Requirements

Parameter	Old SXU Values	New SXU Values
Maximum gap variation	<29 µm	<27 µm
Relative strongback roll	<4 mrad	<4 mrad
Centerline shift due to roll	±478 µm	±500 µm

* This work is supported by the U.S. Department of Energy, Office of Science, Office of Basic Energy Sciences under Contract No. DE-AC02-76SF00515.
† pmallon@lbl.gov

ISBN: 978-3-95450-247-9 ISSN: 2673-5490 doi: 10.18429/JACoW-IPAC2024-MOPC37

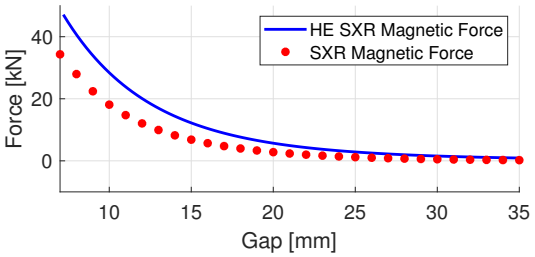

Figure 2: Comparison of SXU and HE-SXU magnetic load per drive system as a function of undulator gap.

Support Frame, Flexures and Strongbacks

The support frame, as its name suggests, must support all operational, thermal, and gravitational loads of the undulator. Moreover, it should be as rigid as possible, since any deflection will have a negative impact on meeting the relevant physics requirements. In the original SXR undulator design, stresses reached a maximum of 20 MPa. Since only the magnetic loads will change with the upgrade to HE, it is assumed that a 30 % increase in load will still fall within reasonable limits.

A finite element model was developed to simulate the mechanical behavior of the flexures and strongbacks under representative loads. The maximum stress due to the magnetic and gravity load seen in the flexures is 93 MPa. The flexures are made from A514 steel, and are assumed to have an average yield stress of 690 MPa. The safety factor for these loads is then 7.4. As with the original SXR undulator design, the maximum stress occurs due to a temperature change of ±15 °C, which leads to a von Mises stress of 254 MPa. This temperature range is what the undulators experience during storage, where they are still required to maintain their calibration. This has been tested extensively through thermal cycling of the currently operational undulators.

Under maximum magnetic load, the gap deflection due to strongback bending is shown to be well below the physics requirement. It is concluded that the strongbacks can be reused without modification. See Fig. 3.

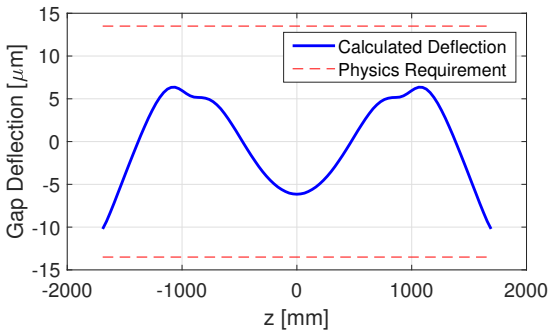

Figure 3: Gap deflection due to strongback bending under maximum magnetic load.

Compensation Springs

The compensation springs are an important complement to the drive system. They allow the system to operate with greatly reduced loads, and contribute to the overall rigidity of the undulator, in particular addressing the roll requirement. Although a variety of force compensation methods can be used, Belleville (disc) springs offer a compact solution in the load range required. Furthermore, a composite spring stack using stacks of springs in series and parallel can be used to approximate the magnetic force curve. In the SXU design, a bilinear spring setup with a "light" spring stack with a lockout feature and a "stiff" spring stack were used between the upper and lower flexures to achieve this. Although a given loading curve for a spring stack does not need to match the magnetic force curve perfectly, it must fall within the "force reversal limit." The upper and lower limits of this envelope correspond to the points at which the springs overcome the vector sum of the magnetic and gravitational forces for the upper and lower strongback assemblies. Excursions outside of this zone are undesirable as they could produce backlash in the drive system.

In order to update to the HE-SXU magnetic force curve (Fig. 2) while minimizing modification and expense, an effort was made to fit the existing footprint. The original SXR undulator design uses 60 mm diameter disc springs for all springs in the stack. The stiff stack uses pairs of springs in parallel. In order to reach the loads needed for HE-SXU and match the desired curve, the thickest springs available in 60 mm diameter would need to be stacked in triplets. With the right lubrication, the hysteresis can be kept low. However, the load on each individual spring of the stiff stack results in a reduced fatigue lifetime. 70 mm diameter springs were therefore considered as replacements for the 60 mm springs, and trials to determine the best lubrication strategies were made. Figure 4 shows data from lubricant testing. This plot is similar to Fig. 5, except zoomed in on the high-load, small gap region. The loading and unloading curves form a hysteresis loop which should be minimized.

A fatigue life estimation is a critical element of compensation spring stack design. A plot comparing the 60 mm and 70 mm spring stacks is shown in Fig. 4. This estimation is based on the lowest (x-axis) and highest (y-axis) loads that an individual spring experiences. [3] The white area represents the well-defined high fatigue life zone, whereas the fatigue life expectancy in the blue zone is unpredictable. The 70 mm springs are shown to be better suited to the load conditions.

The final spring stack configuration consists of three segments. The stiff stack has 13 parallel pairs of 5 mm thick springs in series. It uses a Molykote D-7409 Anti-Friction-Coating with a layer of Loctite 8012 molybdenum paste applied afterwards. The light spring stack has 10 single 4 mm thick springs in series, where each spring has a layer of Loctite 8012 molybdenum paste. The third segment is a custom-designed wave spring, and is used to apply a light preload to the stack and increase margin with respect to the

ISBN: 978-3-95450-247-9 ISSN: 2673-5490 doi: 10.18429/JACoW-IPAC2024-MOPC37

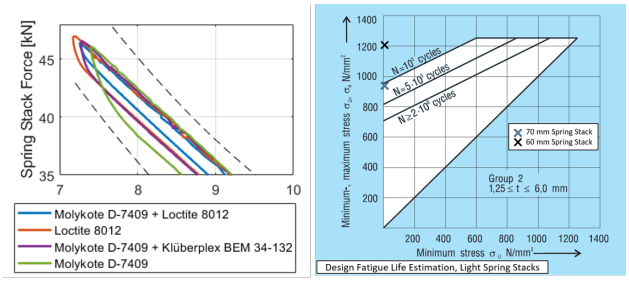

Figure 4: Spring stack hysteresis comparison (left). Fatigue estimation plot for disc springs.

force reversal limit. Figure 5 shows a measured compensation spring stack curve overlaid on the HE-SXU magnetic force curve.

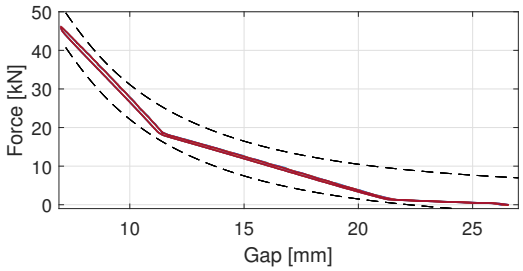

Figure 5: Measured force-displacement curve of a production compensation spring stack.

Since fatigue life and hysteresis were considered to be of great enough importance to merit the use of the larger 70 mm diameter springs stacks, the hard stop support blocks also had to be modified. See Fig. 6, which compares the two designs and shows the final stack arrangement for HE-SXU.

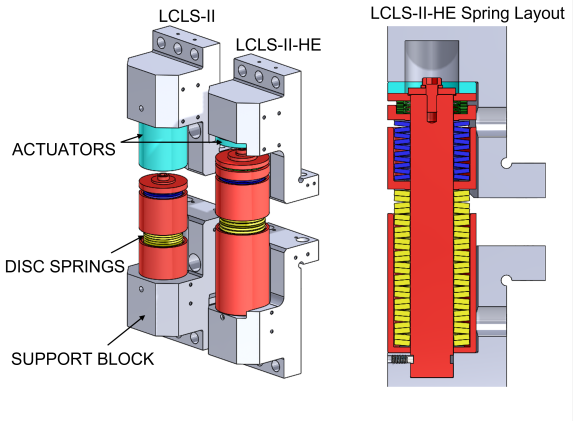

Figure 6: Comparison of SXU and HE-SXU compensation spring stacks (left). Note the modified support blocks.

Since material was planned to be removed from the existing compensation spring support blocks, and due to the increased load passing through them, a finite element model was used to evaluate the stresses and deformations of the modified parts. Due to the way these blocks are attached to the flexures, it was found that they separate from the flexures at minimum gap. It was therefore decided to more substantially modify these parts within the physical design envelope. Further refinements to the design were included to increase rigidity and reduce stress.

Design Validation

In the framework of LCLS-II, the drive system was tested without compensation springs, and the roll was measured to be well within the requirements [4]. To validate the HE-SXU design, an original LCLS-II undulator was reconfigured to the HE configuration and the strongback roll was measured as a function of gap using a laser tracker. The roll was shown to be below 0.75 mrad with a linear response. See Fig. 7.

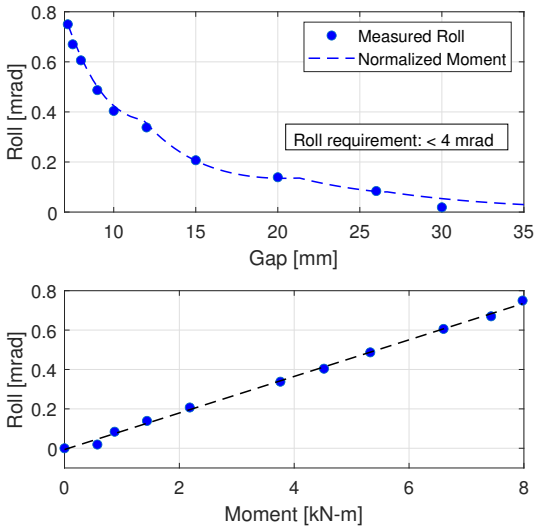

Figure 7: Relative strongback roll as a function of gap and moment.

CONCLUSION

For the undulators of the LCLS-II SXR line, the High Energy upgrade requires that compensation spring stacks be replaced with re-designed units. The in-depth analysis presented in this work yields a robust solution that is implemented with minimal disruption to the existing setup. Additionally, it has been shown through analysis and/or testing that the strongbacks, flexures, drive systems, and frames can be reused without modification.

ACKNOWLEDGEMENTS

The authors would like to acknowledge Troy Stevens and Mark Coleman for their design efforts. Thanks go as well to Michael Hallock and Rae de Leon for their help with compensation spring stack assembly and testing.

REFERENCES

[1] M. Leitner *et al.*, "Hard X-Ray and Soft X-Ray Undulator Segments for the Linear Coherent Light Source Upgrade (LCLS-II) Project", in *Proc. IPAC'17*, Copenhagen, Denmark, May 2017,

ISBN: 978-3-95450-247-9 ISSN: 2673-5490 doi: 10.18429/JACoW-IPAC2024-MOPC37

pp. 1605–1608.
doi:10.18429/JACoW-IPAC2017-TUPAB123

[2] T. O. Raubenheimer, "The LCLS-II-HE, A High Energy Upgrade of the LCLS-II", in *Proc. FLS'18*, Shanghai, China, Mar. 2018, pp. 6–11.
doi:10.18429/JACoW-FLS2018-MOP1WA02

[3] Adolf Schnorr GmbH + Co., *Handbook for Disc Springs*, Heilbronn, Germany, 2003, pp. 24, 92-93.

[4] A. J. DeMello *et al.*, "Engineering Optimization of The Support Structure and Drive System for the LCLS-II Soft X-Ray Undulator Segments", in *Proc. IPAC'17*, Copenhagen, Denmark, May 2017, pp. 1602–1604.
doi:10.18429/JACoW-IPAC2017-TUPAB122